CAD/CAM and Robotics Applications in Laboratory-Learning Environment

R. Radharamanan and Ha Van Vo
School of Engineering, Mercer University, Macon, GA 31207-0001, USA

Abstract

In this paper, how the design/automation hardware and software and manufacturing laboratory facilities are effectively integrated to teach Computer Aided Design (CAD), Computer Aided Manufacturing (CAM), CAD/CAM integration, and robotics with appropriate hands-on experiences in the Biomedical, Mechanical, and Industrial Engineering Programs are presented and discussed. A typical CAD module developed and taught in Biomedical Engineering includes the use of patient-specific 2D computerized tomography (CT) to generate 3D modeling and simulation of the ankle complex using finite element modeling (ANSYS 8.1) for determining the optimal meniscus thickness. Typical lab modules developed and taught in the Mechanical and Industrial Engineering Programs include: 1. The CAD/CAM module: involves designing a spline with 6, 8, or 12 grooves using AutoCAD or Pro-Engineer, making the spline on a CNC machining center using the rotary axis (XZ-plane), measuring certain dimensions of the part made, and making an error analysis; 2. The robot module: involves the use of a programmable five-axis robot (CRS A255) for a Kool-Aid mixing application consisting of designing and building a fixture to hold a cup for Kool-Aid mix, cup for sugar, bottle of water, a mixing cup, and a spoon. The robot arm should be programmed to include all the necessary motions to complete the mixing process. The results obtained from the student team projects on the above three modules are also presented, analyzed, and discussed.

1. Introduction

The advancement of industrial applications of process technology, computers, and automation demands continuous improvement in the quality of engineering education both in classroom theory and in hands-on practice in design, computer simulation, and manufacturing laboratories. There is a growing need for preparing students both in theory and practice so that they are well prepared to meet the challenges of the job market, especially in the manufacturing industries of the 21st century. A strong multi-disciplinary background is required of new engineering graduates because of increased automation and data networking on the shop floor as well as the globalization of most industries. Assessment of student achievement in engineering design is an important part of engineering education and vital to engineering program accreditation. Systematic assessment of design is challenging yet necessary for program improvement.

Several educators, design researchers, and designers from industry have studied and addressed the importance of goals for design engineering education[1], engineering design process[2, 3], design considerations and constraints in the design course sequence[4], visualization skills[5], freshman engineering design[6], and senior capstone design[7, 8].

The objectives of manufacturing engineering education, possible ways of introducing the subject into an undergraduate curriculum, and the urgency for improving it in the educational system that supply industry with engineers have been discussed[9, 10]. Robotics in engineering education1[11, 12] and experiments in part acquisition using robot vision[13] have also been presented and discussed.

At Mercer University School of Engineering (MUSE), the biomedical, mechanical, and industrial engineering students are prepared for careers in manufacturing and service organizations. The students are trained from freshman through senior year in design, materials, manufacturing (CAD/CAM and Robotics), and measurement-related areas.

The design and manufacturing facilities at MUSE include: CAD lab (AutoCAD, Pro/Engineer, and ANSYS) conventional machine shop with lathes, milling, drilling, and grinding machines, welding shop, as well as robotics and automation lab with a 3-axis CNC machining center capable for 4th axis machining, two five-axis robot arms, CNC machines, vision system, and a Coordinate Measuring Machine (CMM) with *PC-DMIS v 3.2* software.

This paper presents some of the laboratory modules developed and taught in the design, biomechanics, manufacturing, and robotics courses at MUSE. Selected results from student team projects are presented, analyzed, and discussed.

2. CAD Module in Biomechanics

This section presents one of the student team projects from biomechanics course: "3D Modeling and Simulation of Ankle Complex". Total ankle arthroplasty has been available since the 1970s[14] and has become a viable treatment for patients with painful tibiotalar arthritis who have not responded well to conservative treatments. It is generally appreciated amongst surgeons who implant artificial joints in the lower extremities, that total ankle replacement (TAR) has been less successful than the replacement of hip and knee. Several factors are considered to be causative in relation to failure of TAR in comparison to total knee and total hip arthroplasty, which include application of greater weight bearing loads (5 times body weight), a smaller surface area (9-11 cm^2) through which the load is dispersed, and greater degrees of freedom (movement) relative to the knee and hip[15, 16]. Recent advances in ankle implant design and availability have increased its popularity. The three most commonly used ankle endoprostheses currently available include the Alvin Agility Total Ankle (AATA) (Deput Orthopedics, Inc., a Johnson & Johnson company, 9140 K-Guilford Rd Columbia, MD 21046), the Buechel-Pappas (BP) (Endotec, 20Valley Street, South Orange, NJ 07079) device, and the Scandinavian Total Ankle Replacement (STAR), W. Link GMBH. & Co, Barkhausenweg 10, D-22339 Hamburg Germany) or Ramses device. Although each of these devices has certain desirable characteristics, they also convey a considerable number of problems that have been noted by other authors[15-17]; among the three, the AATA has been cited as the most popular of the currently available ankle endoprostheses[14, 17].

Every ankle endoprosthesis is subject to failure when malalignment and less than optimal fit is present[18]. Less than optimal fit promotes eccentric loading of the tibial tray and progressive loosening, and therefore implant instability. In addition, these factors also promote excessive wear of the ultrahigh molecular weight polyethylene (UHMWPE) meniscus which ultimately results in implant failure or stress fracture of the supporting bone[18]. Therefore, it is the objective of this study to determine a method to find the optimal solution of implant size and meniscus thickness according to patient specific geometry to improve on surgical outcomes of TAR.

2. 1. 3D modeling and simulation of ankle complex

To conduct the study, a CT scan of a 75-kg white female in her mid-fifties was randomly selected from the Ankle & Foot Care Center of Miami. The patient had previously been conservatively treated during a period of 2 years for painful arthritis of the right ankle. All forms of non-invasive treatments have failed to alleviate the pain. Symptoms of pain along with diminished range of motion have subsequently progressed. Findings from bone x-rays of the right ankle showed signs of degenerative joint disease

(DJD). Surgical treatment via total ankle arthroplasty was addressed and highly recommended to the patient. With patient's consent, a CT scan of the right ankle was obtained to create a 3D FE model. This was done using 180 2-D cross-sectional slices of the CT scan as shown in Fig. 1.

The 3D FE model (Fig. 2) of the ankle complex was then created from the 2D images using ANSYS 8.1 (ANSYS Inc., 275 Technology Drive, Canonsburg, PA 15317). The model was subsequently used to help determine the proper sized ankle prosthesis for the patient by using patient specific geometry. Afterwards, the ankle prosthesis was incorporated into the model to analyze the effects of variable meniscus thickness, bone removal and bone density on contact stresses.

During normal weight bearing, it is understood that the ankle joint supports a load of approximately 5 times the body weight. Therefore, a compressive force along the y-axis of approximately 3,678.75 N was applied constantly to the FE model in order to analyze the contact pressure, δ_{yy} of the ankle joint while in neutral position.

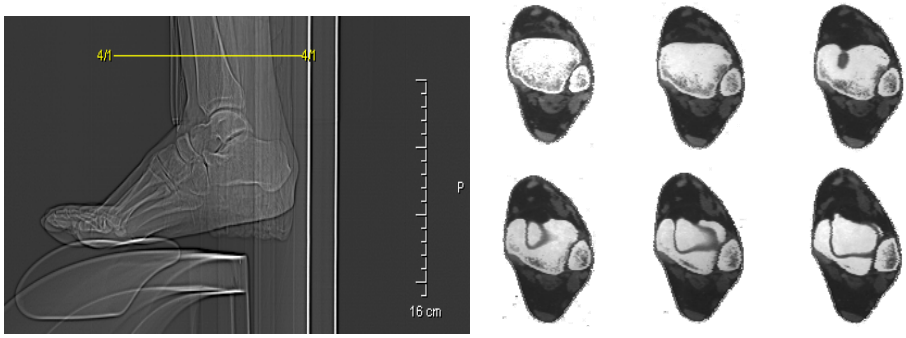

Figure 1. The 2D images generated from the CT scan of the ankle joint.

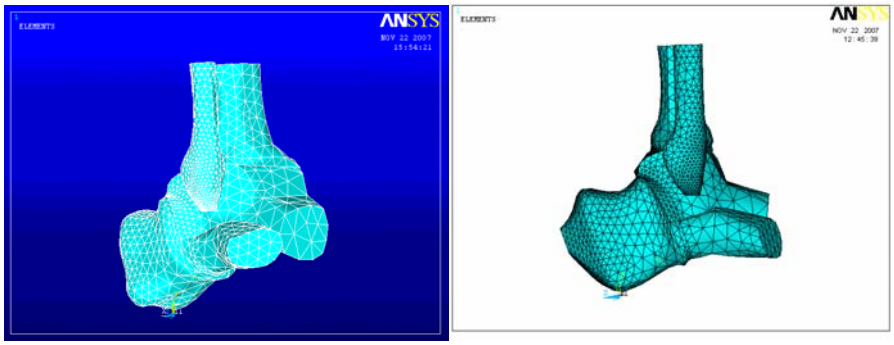

Figure 2. Anterolateral and lateral views of a 3D FE model of the ankle complex.

Contact pressure was examined between the inferior surface of the meniscus and the superior surface of the talar dome. The analysis was simulated in neutral position and in static conditions to eliminate variables such as malalignment and changes in force loads as seen with dynamic conditions.

Simulations were subsequently done for different meniscus thickness. Thickness was increased in 2 mm increments beginning with 2 mm and ending with 12 mm. The thickness was proportional to the thickness of tibial plateau bone removed. Ultimate contact stresses were analyzed and compared. Contact stresses were also determined for variable bone densities and different amounts of tibial bone removed. Data were collected and recorded as shown in Table 1.

Table 1. Data collected applying a load of 5 times the body weight of an average person of 75 kg.

Simulation Run	Applied Loads (N)	Bone Mineral Density (gm/cc)	Ultimate Contact Stress (MPa)	Thickness of Meniscus (mm)	Ultimate Contact Stress (MPa)	Tibial Bone Removal (mm)	Ultimate Contact Stress (MPa)
1	3678.75	0.5	29.698	2	31.269	2	32.135
2	3678.75	0.6	28.753	4	28.494	4	29.037
3	3678.75	0.7	26.995	6	25.394	6	26.504
4	3678.75	0.8	25.771	8	24.861	8	25.107
5	3678.75	0.9	24.927	10	24.850	10	24.105
6	3678.75	1.0	24.027	12	23.889	12	23.889
7	3678.75	1.1	23.386				
8	3678.75	1.2	22.733				

In Table 1, there are one set of eight simulations for computing ultimate contract stress for different bone mineral density and two sets of six simulations for computing ultimate contact stress while varying thickness of meniscus as well as tibial bone removal when a constant 5 times body load was applied.

The optimal thickness came out to be 8.468 mm. These results were found to be comparable to the results of previous studies. In a similar manner, the effect of UHMWPE thickness on contact pressure was described and analyzed by Gur et al[19]. The study was based on the allowable contact stress during compressive loading from 0 to 60 MPa applied to a typical knee design while changing the meniscus thickness from 4 to 24 mm. They concluded that there was an inverse relationship between thickness and contact stress. In addition, the study of Bartel et al[20, 21] also concluded that the stresses were inversely related to the thickness of the polyethylene. A similar study[22] from Orthoteers Company on wear rate of biomaterials determined that thin polyethylene between 6–8 mm in thickness increases fatigue wear and thereafter determined that the thickness level of the meniscus should be between 8–10 mm. So the results from this study are acceptable in terms of the thickness of meniscus for this patient and implant size. It can also be said that the contact stress component is a function of the meniscus thickness.

The common ultimate contact stress for both, the thickness of the tibial bone removal and the thickness of meniscus is 24.986 MPa. The proper size of the implant is dependent on the thickness of the UHMWPE meniscus. The result in Fig. 3 shows that the proper size of the implant is 8.468 mm thickness of the meniscus.

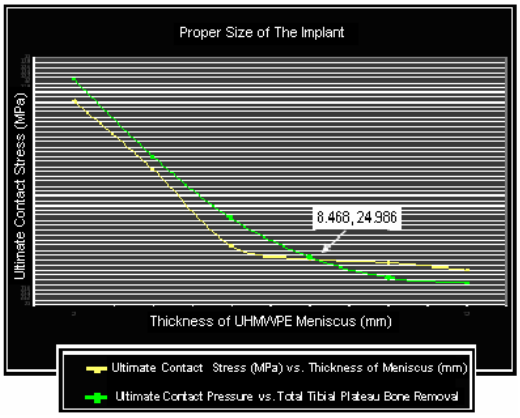

Figure 3. The optimal solution (size of the implant)

Another factor that has a major effect on the ultimate compressive load (contact pressure) and the overall success of the ankle implant is bone density. According to Table 1, bone density has a major effect on contact stress showing an inverse relationship. Lateral views of the new ankle implant experiencing a constant body load is shown in Fig. 4.

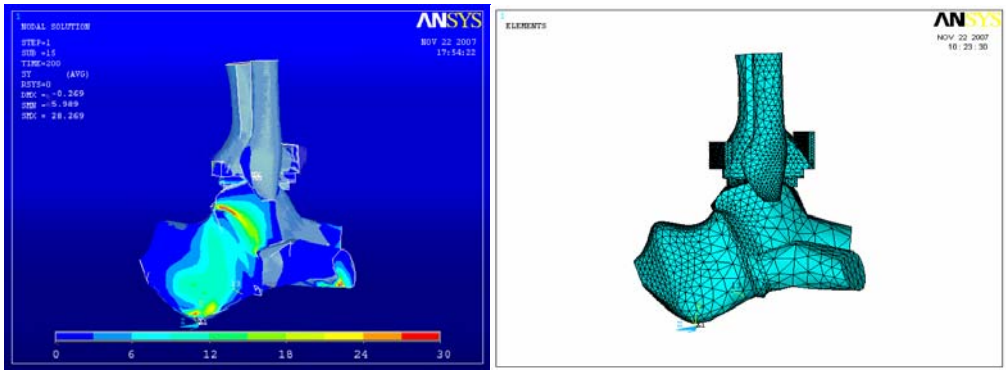

Figure 4. FE model (lateral views) of the new ankle implant experiencing a constant body load of 3678.75 N (5 times body weight of a 75 kg patient).

Previous studies on the effect of thickness of the polyethylene on contact pressure suggested that the thickness of the polyethylene meniscus be between 8–10 mm[20, 21]. In this study, the optimal solution for the thickness of UHMWPE meniscus was 8.468 mm which falls within this range.

3. Design and Fabrication of Spline (DFS Module)

The typical DFS module is part of computer-aided manufacturing course and consists of: (1) Designing a spline with 6, 8, or 12 grooves using one of the design software packages such as AutoCAD or Pro-Engineer; (2) Providing part dimensions and tolerances; (3) Writing the part program in G-code either manually or using Pro-Engineer; (4) Verifying the part program including selection of fixture type, cutting tools, and machining conditions; (5) Using rotary axis (4^{th} axis machining) and CNC machining center for the fabrication of the part including material selection, cutting conditions such as number of grooves, spindle speed, feed, depth of cut, as well as selection of proper milling cutters; (6) Using the dial gage/caliper to measure critical dimensions of the part made such as length, width, and depth of the grooves, taper angle, and outer diameter of the part; (7) Writing a project report covering all aspects of design, fabrication, and measurement of the spline including error analysis.

This module provides the students: (1) The basic understanding of designing a complex shape such as spline; (2) The use of G-codes to program the part designed; (3) Make the part with the help of rotary axis and the CNC machining center; (4) Measure part dimensions using dial gage/caliper; (5) Verify that the measured dimensions are within the specifications and tolerance limits of the part designed, through error analysis.

The design of a typical spline with 12 grooves and the part made are shown in Fig. 5. The part was made using blue wax. The desired dimensions, the tolerance for each dimension and the average of 5 actual measurements of each dimension on one part as well as the absolute percentage error obtained for critical dimensions of the spline designed and fabricated are given in Table 2. The average measurement of each dimension is found to be within the tolerance limit. The Absolute Percentage Error (APE) was calculated using the relation:

$$APE = |(Desired - Actual)/Desired|*100\% \quad (1)$$

The average absolute percentage error for all measured dimensions was found to be less than 2%. The error may be due to work material (blue wax), cutting tool, and improper part set up by the student team.

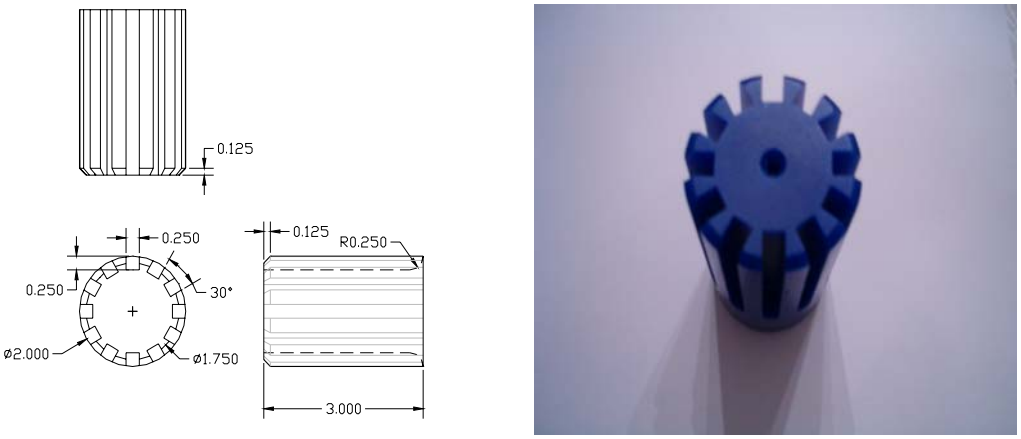

(a) (b)

Figure 5. (a) Design of a spline with 12 grooves; (b) Spline with 12 grooves (part made)

Table 2. Absolute Percentage Error (APE)

Measurement	Desired	Tolerance	Actual	APE
Groove length	2.50 in	± 0.05 in	2.538 in	1.52%
Groove width	0.25 in	± 0.005 in	0.253 in	1.20%
Groove depth	0.25 in	± 0.005 in	0.254 in	1.60%
Chamfer angle	41^o	$\pm 1^o$	41^o	0.00%
Spline length	4.0 in	± 0.05 in	4.02 in	0.50%
Spline diameter	2.0 in	± 0.05 in	2.0332 in	1.66%

4. Kool-aid Mixing

Robotics course is offered in the senior year as an elective course. The CRS A255 robot arm (Fig. 6) has 5 rotational joints and a gripper, utilizes a windows-based software package called *Robocomm3*, and can be manipulated manually using a teach pendant. The operating system used by the *Robocomm3* package is called CROS-500. The language used to program the robot is RAPL-3, which stands for Robot Automation Programming Language. *Robcomm3* allows the users to create and edit robot programs, transfer files between the computer and the controller, and communicate interactively with the controller using the terminal window. A student team in this course programmed the CRS A255 robot arm for the Kool-Aid mixing application. This student project consists of designing and building a fixture to hold a cup for Kool-Aid mix, cup for sugar, bottle of water, a mixing cup, and a spoon. The dimensions for the holes used in the fixture are found in Table 3. The fixture design with the dimensions is shown in Fig. 7. Figure 8 shows the fixture created for mixing Kool-Aid.

Table 3. Dimensions for the Fixture

Hole Characteristics	X Location (in)	Y Location (in)	Dimensions	
			Diameter (in)	Depth (in)
Hole # 1: Mixing cup	2.25	3.00	Ø3.00	↓2.35
Hole # 2: Bottle of water	5.75	3.00	Ø2.875	↓2.25
Hole # 3: Sugar	8.50	2.50	Ø2.00	↓1.30
Hole # 4: Kool-Aid mix	10.68	1.31	Ø1.625	↓0.825

Figure 6. CRS A255 robot arm

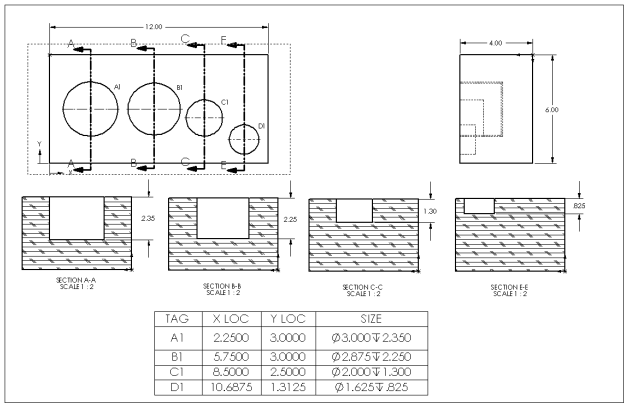

Figure 7. Dimensional drawing of Kool-Aid fixture

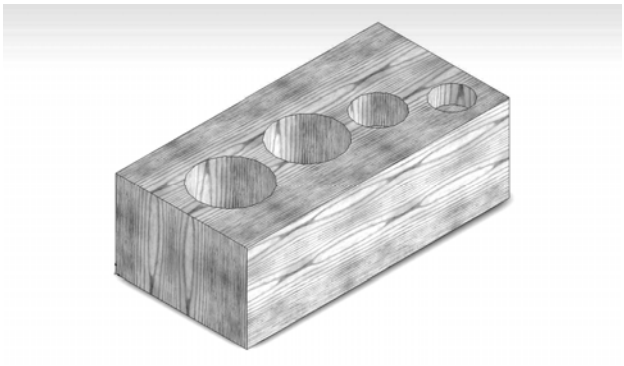

Figure 8. Kool-Aid fixture

The next step in the process was to create a work cell for the fixture to be located during the process of making the Kool-Aid. The fixture was placed directly in the center of the table in front of the robot. The Kool-Aid making process was broken down into four main stages: add mix, add sugar, add water, and stir with a spoon. Each stage has its own set of positions, speeds, and movements that allow for the completion of the Kool-Aid drink.

The complete mixing process included the following robot motions: pick-up the Kool-Aid mix, pour the Kool-Aid mix into the cup, return the mix cup to the initial location, pick up the sugar cup, pour the sugar into the mixing cup, return the sugar cup to the initial location, pick up the cover on top of the water bottle, place the cover on the table, pick up the water bottle, pour the water into the mixing cup, return the bottle to the initial location, pick up the spoon, stir the spoon in the Kool-Aid mixture, and return the spoon to the initial location. The Kool-Aid process flow diagram is shown in Fig. 9. Once the robot was programmed, the final step was to run the program and observe the results. The robot was able to make a cup of Kool-Aid in approximately 3 minutes. The program was then perfected through subsequent trials,

the final process was videotaped. The video was then edited using the software iMovie and will be shown during the presentation.

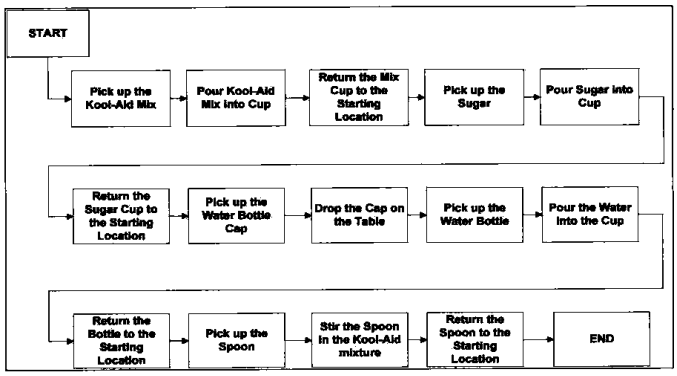

Figure 9. Kool-Aid process flow diagram

5. Conclusions

The biomedical, mechanical, and industrial engineering curriculum at MUSE provides significant learning opportunities to the students. Theory on design, 3D modeling and simulation, manufacturing, automation, and robotics span the curriculum. Hands-on experience in design and manufacturing laboratories, and open-ended design projects from freshman through senior years reinforce the theory. Lastly, Students participate in real world experience through industry co-op, summer internship, and participation in professional society activities. Typical examples of laboratory work (CAD, CAD/CAM, and robotics modules) developed, presented and discussed in this paper clearly indicate the learning opportunities provided to the students at MUSE. The students also participate in the multidisciplinary senior design projects in their final year. The effective use of theory classes, design and manufacturing lab facilities, multidisciplinary senior design projects, and co-op opportunities provide the students the needed expertise and prepare them well to meet the challenges in the industrial workplace.

References

[1] Davis, D. C., Gentili, K. L., Trevisa, M. S., and Calkins, D. E., "Engineering Design Assessment Processes and Scoring Scales for Program Improvement and Accountability," *Journal of Engineering Education*, Vol. 91 (No. 2), 2002, pp. 211-221.

[2] Dym, C. L., Sheppard, S. D., and Wesner, J. W., "A Report on Mudd Design Workshop II: Designing Design Education for the 21st Century," *Journal of Engineering Education*, Vol. 90 (No. 3), 2001, pp. 291-294.

[3] Haik, Y. *Engineering Design Process*, Thomson Books/Cole, CA, 2003.

[4] Koehn, E., "Preparing Students for Engineering Design & Practice", *Journal of Engineering Education*, Vol. 88 (No. 2), 1999, pp. 163-167.

[5] Sorby, S. A., and Baartmans, B. J., "The Development and Assessment of a Course for Enhancing the 3-D Spatial Visualization Skills of First Year Engineering Students," *Journal of Engineering Education*, Vol. 89 (No. 3), 2001, pp. 301-307.

[6] Barr, R. E., Schmidt, P. S., Krueger, T. J and Twu C-Y., "An Introduction to Engineering Through and Integrated Reverse Engineering and Design Graphics Project," *Journal of Engineering Education*, Vol. 89 (No. 4), 2000, pp. 413-418.
[7] Moor, S. S., and Drake, B. D., "Addressing Common Problems in Engineering Design Projects: A Project Management Approach", *Journal of Engineering Education*, Vol. 90 (No. 3), 2001, pp. 389-395.
[8] Sheppard, S. D., "Design as Cornerstone and Capstone," Mechanical Engineering Design, November, 1999, pp. 44-47, New York, NY.
[9] Swearengen, J. C., Barnes, S., Coe, S., Reinhardt, C., and Subramanian, K., "Globalization and the Undergraduate Manufacturing Curriculum," *Journal of Engineering Education*, Vol. 91 (No. 2), 2002, pp. 255-261.
[10] Todd, R. H., Red, E.W., Magleby, S. P., and Coe, S., "Manufacturing: A Strategic Opportunity for Engineering Education,"*Journal of Engineering Education*, Vol. 90 (No. 3), 2001, pp. 397-405.
[11] Walter, W. W., "Undergraduate Robotics Education on a Shoestring," *Proc. 2nd International Conference on Robotics and Factories of the Future,* 1987, pp. 807-815.
[12] Jeswiet, J., "Robots in Education," *Proc. ASME International Computers in Engineering Conference,* Vol. II, Boston, 1985, pp.445-449.
[13] Nagel, R, Vanderberg, G., Albus. J., and Lowerfeld, E., "Experiments in Part Acquisition using Robot Vision," *Robotics Today,* Windter, 1980-81, pp.30-35.
[14] Corti S. F., et al, "Complications of Total Ankle Replacement", 1(391), pp. 105-114, October 2001.
[15] Felman, M. M., "The Total Ankle Joint Replacement", Study 98-99.
[16] Felman, M. M., "This Surgical Procedure Became Available to Americans in October of 1998", wysiyg://result-doc-frame.content, 2000.
[17] L. Claes L., Eberhard, O., and Bauer G., "Engineering Considerations of a New Ankle Joint", http://www.cmmaccess.com, January 1999.
[18] Raikin, S. M., and Myerson, M. S., "Complications of Total Ankle Replacement", pub/pressItem73.html. http://www.drmyerson.com/research
[19] Gur, H., Aktiengesellschaff, H., and Kunstoffe V., 6230 Frankfurt am Main 80, 1982, p. 22.
[20] Bartel D. L., et al, "The Effect of Conformity and Plastic Thickness on Contact Stresses in Metal Backed Plastic Implants", Journal of Biomechanical Engineering, 107, 1985, p. 193-199.
[21] Bartel, D. L., Bicknell V. L., and Wright T. M., "The Effect of Conformity, Thickness, and Material on Stresses in Ultra-High Molecular Weight Components for Total Joint Replacement", Clinical Orthopaedics and Related Research, 68-A (7), 1986, p. 1041-1051.
[22] Implants & Materials in Orthopedics, http://www.orthoteers.co.uk/Nrujpij33Lm/Orthbiomat.htm.

Biography

R. Radharamanan: Dr. R. Radharamanan is a professor in the Department of Mechanical and Industrial Engineering at Mercer University in Macon, Georgia. He has thirty five years of teaching, research, and consulting experiences. His previous administrative experiences include: President of International Society for Productivity Enhancement (ISPE), Acting Director of Industrial Engineering as well as Director of Advanced Manufacturing Center at Marquette University, and Research Director of CAM and Robotics Center at San Diego State University. His primary research and teaching interests are in the areas of manufacturing systems (CAD/CAM and Robotics), modeling and simulation, quality engineering, and product and process development. He has organized and chaired/co-chaired five international conferences on CAD/CAM, Robotics and Factories of the Future, and organized and chaired one regional seminar on Operations Research. He has received two teaching awards, several research and service awards in the United States and in Brazil. His professional affiliations include ASEE, IIE, ASQ, SME, ASME, and ISPE.

Ha Van Vo: Dr. Ha Van Vo is an Assistant Professor in the Department of Biomedical Engineering and Physician, Mercer University, Macon, GA. His main teaching and clinical research focus on sport medicine biomechanics, accidental injury biomechanics, rehabilitation engineering, medical devices, laser guide for surgery, orthopedic implants, and biomedical materials.